

Magnetic Properties of Al-Co-N Thin Films Dispersed with Co Particles

Chang-Suk Han[†]

Dept. of Defense Science & Technology, Hoseo University,
165 Sechul-Ri, Baebang-Myun, Asan City, Chungnam 336-795, Korea

Abstract Al-Co-N thin films, Al-Co-N/Al-N and Al-Co-N/Al-Co multilayers containing various amounts of Co content were deposited by using a two-facing targets type dc sputtering (TFTS) system. The films were also annealed successively and isothermally at different annealing temperatures. Irrespective of Co content and preparation methods, all the as-deposited films were observed non-magnetized. It was found that annealing conditions can control the magnetic and electrical properties as well as the microstructure of the films.

(Received December 3, 2007; accepted January 11, 2008)

Key words: Composite target, Al-Co-N, Al-Co, saturation magnetization, thin films, multilayer films

1. Introduction

Recent high technology developments of electronic devices have led to a demand for miniaturization of magnetic devices [1], operating at frequencies higher than 50 MHz. For that aim, micromagnetic devices using thin film inductors or transformers operating at high frequency have been proposed [2]. For such devices, it is required that the magnetic materials have a sufficiently large electrical resistivity ρ and are in the form of thin films, to suppress eddy current losses. In the field of magnetic recording, ferrite heads connected with oxide media have been in great use for a long period of time. On the other hand, metal heads [3, 4], for use with high Hc metal media [5, 6] utilizing metallic materials such as metal sendust and single-phase amorphous films have also been introduced in order to achieve high-density recording. There exists a great deal of core loss in high frequency range. However, ferrite heads have a related problem when applied to high-density technology, that is, the low Bs of soft magnetic ferrite makes them incompatible with metal media. In order to solve those two major problems,

high resistive metal films possessing a very fine two-phase hetero-amorphous structure have been studied, and magnetic granular system, where the magnetic particles are embedded in an insulator matrix, has also been studied. Moreover, it was found that multilayer films show better soft magnetic properties than monolayer films [7, 8]. But it is necessary to improve the overall performance of the high density recording materials. Few works have been reported till now on Co based soft magnetic materials, where Co as a magnetic element is embedded in a good insulating matrix. An ideal high-density recording magnetic material should have high permeability, high electrical resistivity, large saturation magnetization coupled with low energy loss and also a high corrosion resistance. That is why we used AlN as a high resistive and high corrosion resistance insulator matrix and Co as a magnetic particle embedded or dispersed in that matrix.

In this paper, we describe the processing of Al-Co-N thin films, Al-Co-N/Al-N and Al-Co-N/Al-Co multilayer films containing various amounts of Co content and also examine their magnetic and electrical properties in relation to the microstructure of the films.

[†]E-mail : hancs@hoseo.edu

2. Experimental procedure

Aluminum nitride (AlN) thin films were deposited on glass substrate by using a two facing targets type d.c. sputtering (TFTS) system [9, 10] at various nitrogen partial pressures (P_{N_2}). Their deposition characteristics, crystallographic orientation and also microstructure were examined to determine the best deposition condition. Thus predetermined conditions were applied to prepare Al-Co-N thin films by only replacing an aluminum target by an 'Al-Co' composite target in this system. The composite target was fabricated by insetting a Co plate with various diameters into a hole cut in the central part of Al target. In this system, a pair of permanent magnets are

installed behind both targets, as shown in Fig. 1. The magnetic field from these magnets confines the plasma between the two targets. Consequently, the films can grow without disturbance from plasma because the substrate is located out of the plasma. The deposition conditions for Al-Co-N thin films are listed in Table 1. Al-Co-N/Al-N multilayer films were prepared by only regulating the bias voltage. During the deposition of Al-N layer total pressure and bias voltage were adjusted to 1 Pa and -900 V respectively, and the sputtering current was only 0.01-0.02 mA. Al-Co-N/Al-Co multilayer films were fabricated by using Ar and (Ar + N_2) mixture alternatively. As-deposited films were annealed isothermally in a vacuum of 2.6×10^{-4} Pa at different temperatures. The microstructure of thus prepared films was examined by X-ray diffraction (XRD), transmission electron microscope (TEM). Atomic percentage of the contents of the films was checked by energy dispersive spectroscopy (EDS), as listed in Table 2. Magnetic and electrical properties

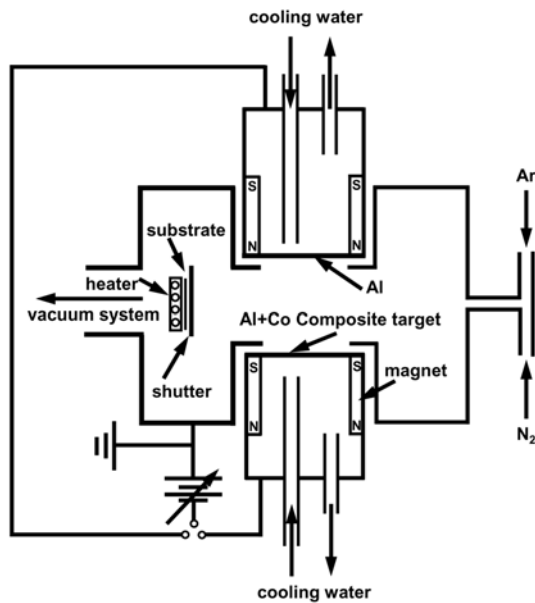


Fig. 1. Schematic diagram of a TFTS system.

Table 1. Deposition conditions

| Target | Al(99.95), Co(99.98) |
|-----------------------|--|
| Composite Target | Area ratio of Co (TAF) $Co/(Al + Co) = 0.021, 0.047, 0.087$ |
| Substrate | Glass, Corning glass (7059), NaCl |
| Substrate Temperature | Lower than 50°C |
| Target Voltage | DC 300 V to 500 V |
| Sputtering Current | 400 mA |
| Composite Gas | N_2 partial gas pressure of 0.52 |
| Initial Pressure | Lower than 2×10^{-4} Pa |
| Total Gas Pressure | 0.4 Pa |

Table 2. Properties of as-deposited films

| Kind of film | TAF of Co (Co at% (approx.)) | Magnetization emu/cm ³ | Resistivity $\mu\text{-}\Omega\text{-cm}$ |
|----------------------------|------------------------------|-----------------------------------|---|
| Al-Co-N | 0.021 (10 at%) | 2.0 ~ 5.0 | 4500 ~ 5000 |
| Al-Co-N | 0.047 (20 at%) | 3.5 ~ 5.0 | 2500 ~ 2900 |
| Al-Co-N | 0.087 (25 at%) | 1.5 ~ 6.0 | 990 ~ 1360 |
| Al-Co-N/Al-N (multilayer) | 0.087 | 0.5 ~ 1.7 | 2700 ~ 2800 |
| Al-Co-N/Al-Co (multilayer) | 0.087 | 1.5 ~ 3.0 | 500 ~ 650 |

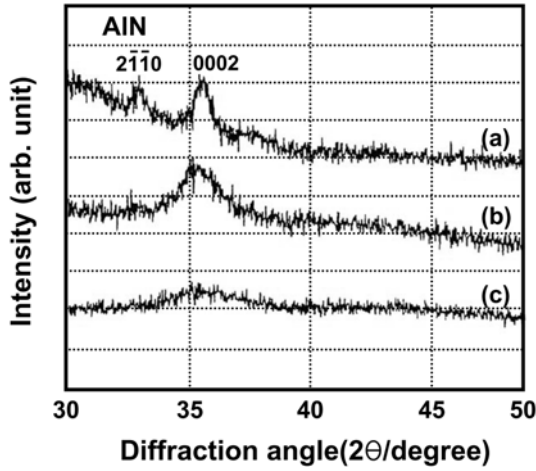


Fig. 2. XRD profiles of as-deposited films containing Co at% of (a) 10, (b) 20 and (c) 25.

were examined by a vibrational sample magnetometer (VSM) and the four probe method respectively.

3. Results and Discussion

3.1 As-deposited films

3.1.1 Microstructure and crystallinity

- Al-Co-N thin films

The microstructure of Al-Co-N films strongly depends of Co content in the films. Fig. 2 shows X-ray diffraction profiles deposited with different Co target area fractions ($\text{Co}/(\text{Co} + \text{Al}) = \text{TAF}$).

For the films prepared with a $\text{TAF} = 0.021$, only two AlN peaks are observed. These AlN peaks are not sharp and are shifted to smaller angle side, which suggests that some of N atoms in the AlN structure are substituted by Co atoms to form a defected AlN crystal structure. For such films prepared with higher TAF's, AlN 0002 peak becomes broad with increasing Co content, and finally disappears in diffuse scattering ascribed to amorphous state.

The results of TEM observations (shown in Fig. 3) are consistent with the XRD results. As shown in the photos, the grain size decreases

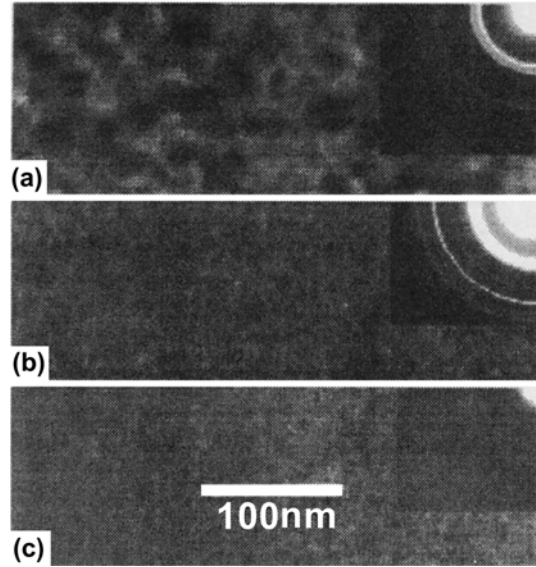


Fig. 3. TEM images and SAED patterns of Al-Co-N films containing Co at% : (a) 10, (b) 20 and (c) 25.

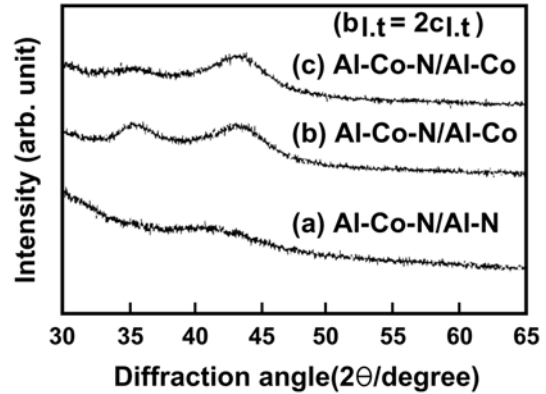


Fig. 4. XRD profiles of as-deposited multilayer films.

with increasing Co content, and corresponding electron diffraction pattern shows only the AlN rings for the film containing 10 at% Co. The films with higher Co contents show that the grain size decreases and the diffraction rings diffuse with increasing Co content.

- Al-Co-N/Al-N and Al-Co-N/Al-Co multilayer films

Fig. 4 shows that Al-Co-N/Al-N films are amorphous but Al-Co-N/Al-Co multilayer shows two broad peaks around the angular position of

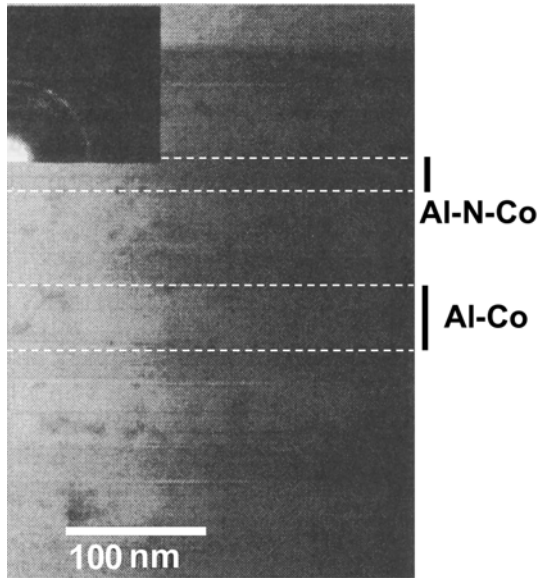


Fig. 5. TEM X-sectional image and SAED pattern of as-deposited Al-Co-N/Al-Co multilayer film.

AlN and Co, and all the peaks are relatively broader for thinner layer thicknesses. The appearance of alternative stacking of Al-Co-N/Al-Co multilayer deposited in as-deposited state is clear as shown in Fig. 5. The inset shows a SAED pattern supporting the XRD results described above.

3.1.2 Magnetic and electrical properties

For all the as-deposited films (Al-Co-N, Al-Co-N/Al-N, Al-Co-N/Al-Co), the saturation magnetization is too small irrespective of Co content. This may be due to the fact that the as-deposited films are amorphous i.e., Co is not in crystalline state, and/or its Curie temperature decreases below room temperature. The resistivity decreases with increasing Co (and Al in case of multilayer films) content of account of the increase of conducting element in the matrix. The numerical results for magnetization and resistivity with respect to Co content in the films are listed in the Table 2.

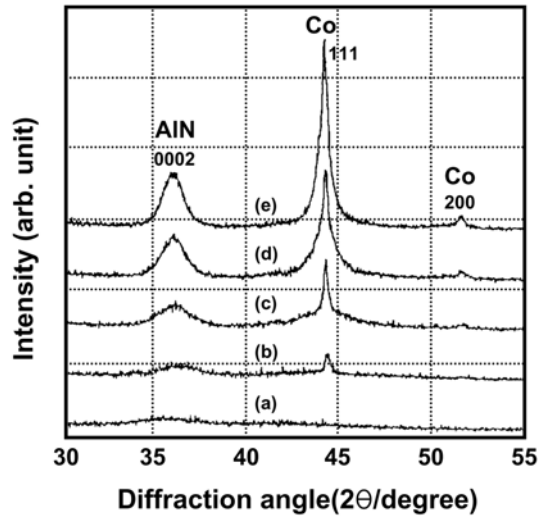


Fig. 6. XRD profiles of Al-Co-N films (TAF = 0.087); (a) as-deposited and (b), (c), (d), (e) annealed at 673 K, 773 K, 873 K, 973 K for 10.8 ks.

3.2 Annealed films

3.2.1 Microstructure and phase separation

Fig. 6 shows some XRD profiles of Al-Co-N films deposited on glass substrate with TAF = 0.087, successively annealed at various temperatures for 10.8 ks at every step. It is clear from the profiles that the amorphous phase of as-deposited film separates into two distinct phases of AlN and fcc Co, and the peak intensity and sharpness increase with increasing annealing temperature.

Fig. 7 shows three typical TEM micrographs of films containing 25 at% Co. The films were successively annealed at various temperatures for 7.2 ks. It is obviously seen that the grain size increases with increasing annealing temperature and the diffuse electron diffraction rings become sharper with increasing annealing temperature. When the film was annealed at 973 K, sharp rings for both AlN and fcc Co were clearly observed. It was also found that the Co grain size was much larger than the AlN grain size at elevated temperatures, especially for the films with higher Co contents. The average Co

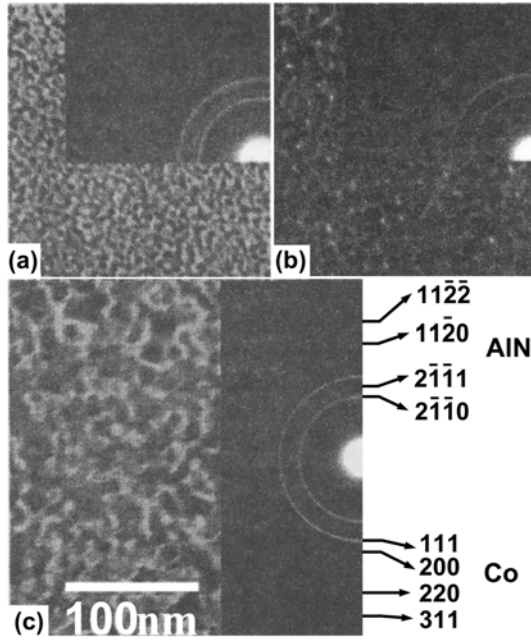


Fig. 7. TEM images and SAED patterns of Al-Co-N films with TAF = 0.087; annealed at (a) 773 K, (b) 873 K and (c) 973 K for 7.2 ks.

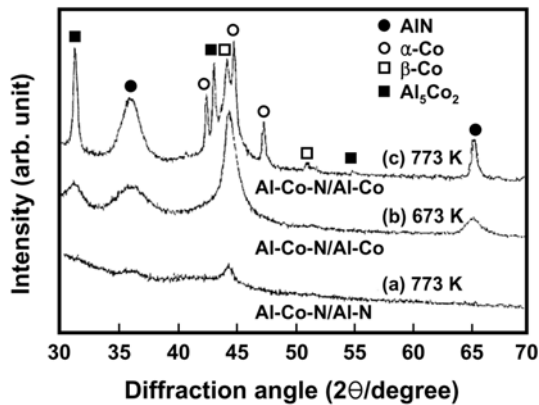


Fig. 8. XRD profiles for annealed multilayer films.

grain size is about 15 nm in diameter and AlN grain size is about 5 nm in diameter for the films containing 25 at% Co annealed at 973 K. The same results were also obtained for isothermal annealing.

Fig. 8 shows XRD profiles of Al-Co-N/Al-N and Al-Co-N/Al-Co multilayer films deposited on glass substrate and annealed at different temper-

atures isothermally for 120 ks. Al-Co-N/Al-N multilayer shows almost the same behavior as Al-Co-N thin films. It crystallizes into two phases of Al and Co at 773 K. On the other hand, in case of Al-Co-N/Al-Co multilayer films, crystallization starts at about 573 K. When annealed at 673 K three phases of AlN, Al_5Co_2 and $\beta\text{-Co}$ are detected, but when annealed at 773 K, they crystallize into four distinct phases of AlN, Al_5Co_2 , $\beta\text{-Co}$ and $\beta\text{-Co}$. The results are summarized as follows; heat treatment can change the microstructure, as-deposited Al-Co-N films, and Al-Co-N/Al-N multilayer films can crystallize to have two distinct phases of AlN and $\beta\text{-Co}$. But, Al-Co-N/Al-Co multilayer films crystallize into four distinct phases of AlN, $\alpha\text{-Co}$, $\beta\text{-Co}$ and Al_5Co_2 .

3.2.2 Magnetic properties and annealing conditions

The magnetic properties of annealed films change in accordance with the changes in microstructure. Fig. 9 shown the saturation magnetization as a function of the annealing time at different annealing temperatures for the films prepared with TAF = 0.087. The saturation magnetization is mainly dependent on annealing temperature and is scarcely affected by annealing time after 20 ks except for the plots at 573 K (Fig. 9(a)), where the increasing tendency of saturation magnetization with increasing annealing time was seen up to 129.6 ks and the highest saturation magnetization of 370 emu/cm^3 was obtained for a film annealed at 773 K for 32.4 ks. The highest saturation magnetization of about 400 emu/cm^3 was obtained for a Al-Co-N/Al-N multilayer film (Fig. 9(b)) annealed at 773 K for 120 ks. This phenomenon can be explained in terms of the changes in microstructure caused by annealing. As annealing time and temperature increases the separation of Co phase from Al-Co-N amorphous phase becomes more dominant,

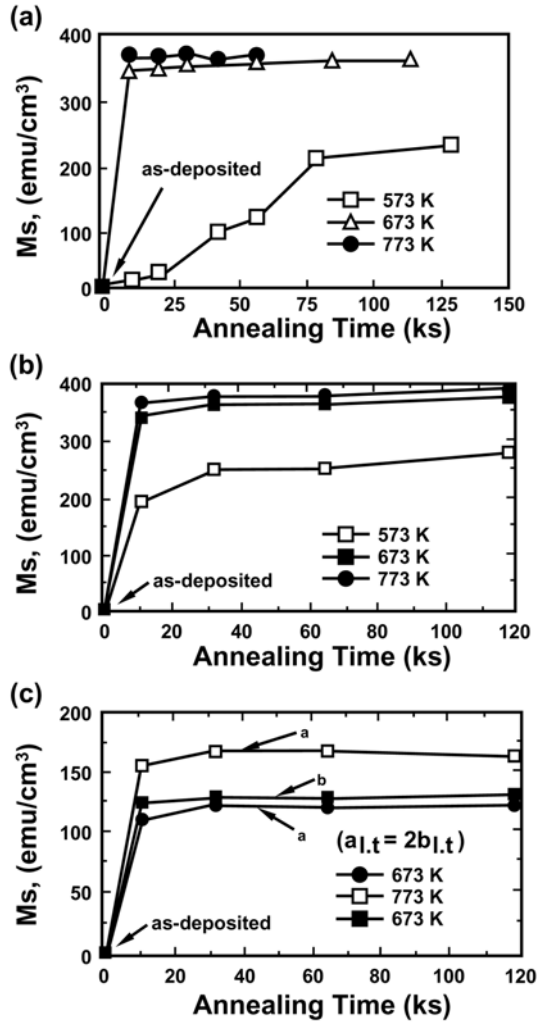


Fig. 9. Saturation magnetization of the films prepared with $\text{TAF} = 0.087$; (a) Al-Co-N, (b) Al-Co-N/Al-N and (c) Al-Co-N/Al-Co.

and the crystallinity of Co becomes more and more perfect. The Co phase dispersed in the AlN matrix leads to the increase of magnetization in the film. In contrast to this, the saturation magnetization of Al-Co-N/Al-Co multilayer films is relatively smaller. A highest value of about $170 \text{ emu}/\text{cm}^3$ was obtained for this kind of films when annealed at 773 K (Fig. 9)). This low saturation magnetization is attributed to the formation of Al_5Co_2 compound; the magnetic moment of which is much lower than that of Co.

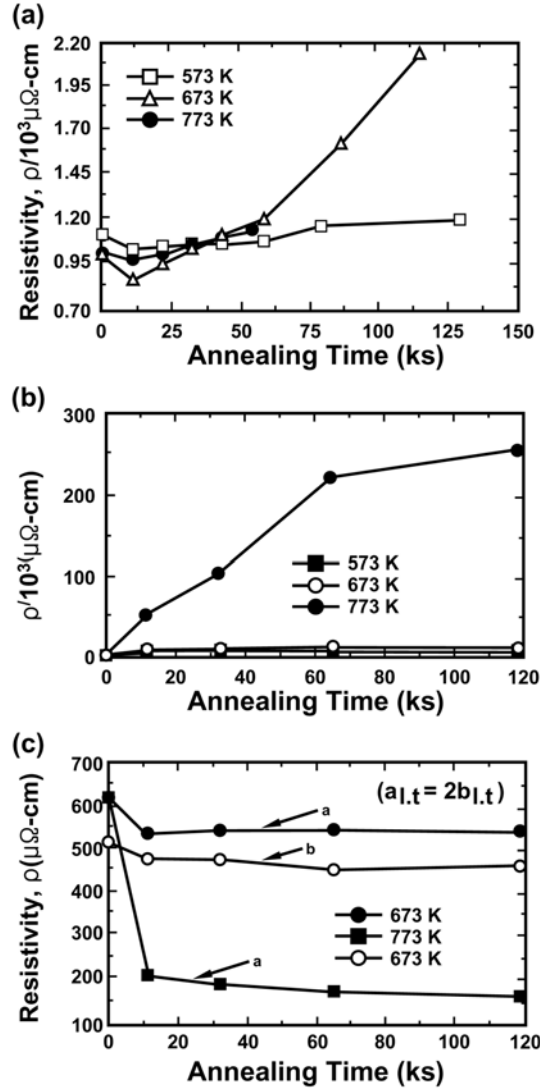


Fig. 10. Resistivity of the films prepared with $\text{TAF} = 0.087$; (a) Al-Co-N, (b) Al-Co-N/Al-N and (c) Al-Co-N/Al-Co.

3.2.3 Resistivity

The resistivity of Al-Co-N thin films, Al-Co-N/Al-N and Al-Co-N/Al-Co multilayer films were also examined for isothermal annealing. For Al-Co-N thin films resistivity first decreases up to 12 ks and then increases with increasing annealing time and temperature (Fig. 10(a)). The decrease in resistivity during the initial stage of annealing is probably due to the evaporation of few atomic

Table 3. Properties of annealed films

| Kind of film | TAF of Co (Co at%(approx.)) | Magnetization emu/cm ³ | Resistivity μ - Ω -cm |
|----------------------------|-----------------------------|-----------------------------------|----------------------------------|
| Al-Co-N | 0.021 (10 at%) | - | - |
| Al-Co-N | 0.047 (20 at%) | ~ 260 | ~ 11×10^5 |
| Al-Co-N | 0.087 (25 at%) | ~ 360 | ~ 2200 |
| Al-Co-N/Al-N (multilayer) | 0.087 | ~ 395 | ~ 25×10^4 |
| Al-Co-N/Al-Co (multilayer) | 0.087 | ~ 160 | ~ 625 |

N atoms before the formation of AlN compound. For Al-Co-N/Al-N multilayer the resistivity increases with increasing annealing time and temperature and the increment is steep at higher temperatures (Fig. 10(b)). The highest resistivity of about 250 Ω -cm was obtained for a film annealed at 773 K for 12 ks. The steep rise in resistivity is due to the dominant crystallization and separation of Co phase from AlN and/or Al-Co-N amorphous phase. In contrast to that, for Al-Co-N/Al-Co multilayer films, resistivity decreases with increasing annealing temperatures, and the decrement is sharp for higher temperatures (Fig. 10 (c)). This is due to the formation of Al₅Co₂ compound which makes a connecting network with Co particles and the rapid formation rate of Al₅Co₂ compound at higher temperatures is also concerned with this. The properties of annealed films are tabulated in Table 3.

4. Conclusions

Amorphous Al-Co-N films deposited by the TFTS system and a new approach were introduced for preparing Al-Co-N/Al-N and Al-Co-N/Al-Co multilayer films. Deposited films were annealed and their microstructure, magnetic properties and resistivity were investigated. The main results are summarized as follows :

1. This TFTS method is suitable for preparing AlN thin films containing various amounts of Co

content and also for preparing multilayer films.

2. Annealing can control the physical properties as well as the microstructure of the prepared films.

3. The magnetization and resistivity are obtainable in Al-Co-N/Al-N multilayer films among these three types of films. Films having such considerable magnetization and resistivity are a potential candidate to be used as a high density recording material.

References

1. R. F. Sooho : IEEE. Trans. Magn., **25** (1989) 1803.
2. K. I. Arai and M. Yamaguchi : J. Magn. Soc. Jpn. **27** (2003) 642.
3. T. Kobayashi, M. Kubota, H. Satoh, T. Kamura, K. Yamauchi and S. Takahashi : IEEE Trans, Magn. **MAG-31** (1995) 1536.
4. J. S. Fang, L. C. Yang, C. S. Hsu, G. S. Chen, Y. W. Lin and G. S. Chen : Journal of Vacuum Science & Technology, **22** (2004) 698.
5. H. Shibaya and I. Fukuda : IEEE Trans. Magn. **MAG-33** (1997) 1005.
6. R. Chubachi and N. Tamagawa : IEEE Trans. Magn. **MAG-30** (1994) 45.
7. K. Asami, S. Ohnuma and T. Masumoto : Surface and Interface Analysis, **26** (1998) 659.
8. N. X. Sun, S. X. Wang, C. Y. Hung, C. X. Chien and H. C. Tong : Materials Research Society Symposia Proceedings, **614** (2001) 2.
9. C. S. Han and O. Nittono : J. Kor. Inst. Met & Mater. **39** (2001) 253.
10. C. S. Han and O. Nittono : J. Kor. Inst. Met & Mater. **39** (2001) 747.